The influence of the cooling rate on the glass transition and the glassy state in three-dimensional dense polymer melts: a Monte Carlo study

1993 J. Phys.: Condens. Matter 5 1597

(http://iopscience.iop.org/0953-8984/5/11/002)

J. Phys.: Condens. Matter 5 (1993) 1597–1618. Printed in the UK

The influence of the cooling rate on the glass transition and the glassy state in three-dimensional dense polymer melts: a Monte Carlo study

Jörg Baschnagel†, K Binder† and H-P Wittmann‡

† Institut für Physik, Johannes Gutenberg-Universität, Staudinger Weg 7, D-6500 Mainz, Federal Republic of Germany

‡ Department of Chemical Engineering, University of California, Santa Barbara, CA 93106, USA

Received 24 August 1992, in final form 15 December 1992

Abstract. In this Monte Carlo simulation we study the glass transition of a dense three-dimensional polymer melt using a lattice model (a bond-fluctuation model on a simple cubic lattice) that was highly optimized for a vector supercomputer. Long bonds are energetically favoured to create a competition between bond energy and packing constraints, which prevents the melt from crystallizing when it freezes. The onset of this freezing can be monitored by the temperature variation of various static quantities that probe both the length scale of a bond vector, such as the mean bond length and mean energy per bond, and that of the whole chain, such as the radius of gyration. As the melt vitrifies, these quantities gradually become independent of temperature in a narrow range around $T \approx 0.2$ (the temperature is measured in units of an energy parameter, ϵ, introduced in the model Hamiltonian) and their value at low temperatures is strongly influenced by the cooling rate. It is thus possible to infer from these curves the cooling-rate dependence of the freezing temperature T_g. This analysis, which was done for fourteen different cooling rates covering two decades, shows that T_g does not necessarily vary linearly with the logarithm of the cooling rate, but can also be well described by a 'Vogel–Fulcher' type of equation, giving a freezing temperature of $T_K \approx 0.17$ at an infinitely slow cooling rate. The type of cooling-rate dependence of T_g that is found depends upon the physical quantity from which it is derived and upon the size of the studied temperature and cooling-rate interval. Despite the difference in the detailed dependence of T_g on the cooling rate, the extrapolated value T_K coincides with the Vogel–Fulcher temperature T_0, obtained from the temperature variation of the diffusion coefficient, within the error bars.

1. Introduction

Although a lot of experimental and theoretical work has been done in order to elucidate the physical phenomenon of the glass transition [1,2], the theoretical description of this transition must still be looked upon as an unsolved question [1,3]. Motivated by the experimental finding of a rather pronounced discontinuity of the specific heat at constant pressure, or of the thermal expansion coefficient, and by the 'Kauzmann' paradox [4], it was speculated that there is an underlying thermodynamic glass transition of second order that is blurred by the finite experimental observation time [5,6]. In the respective theories the glass transition is related to the vanishing of a

0953-8984/93/111597+22$07.50

percolation path for the 'free volume' around a molecule [6] or of the configurational entropy [5]. Although it is possible to understand the empirical Vogel–Fulcher law [7] within the framework of these thermodynamic theories, they cannot account for the detailed dynamical aspects of the glass transition [1]. However, a detailed explanation of these aspects has been attempted by an extension of the mode-coupling theory [8] to the glass transition, which in its idealized version [2] views this transition as a purely dynamical phenomenon where the characteristic timescales of the glass-forming system diverge when a critical temperature is approached without any simultaneous divergence of a length scale. This critical temperature is situated in the region of the undercooled liquid and is thus well above the calorimetric glass-transition temperature. Therefore both the static and dynamical approaches to the glass transition predict that the glass-forming system loses its mobility at a certain temperature, whereas an unprejudiced look at the temperature variation of the viscosity supplies no evidence for a sudden change. Rather, the viscosity varies smoothly with temperature, changing slope around 10^2 poise [1,9] and then increasing dramatically to such large values upon cooling the supercooled fluid that the associated relaxation times become macroscopic (i.e. $1–10^3$ s, or larger). Hence it is inevitable to have a gradual freezing process during which the glass former falls out of equilibrium when the internal relaxation times of the system become comparable to the experimental observation time, i.e. the cooling rate [3, 10]. The crucial role of the correct choice of the cooling rate in the preparation of a glass in order to bypass crystallization is well known from both experiments and computer simulations. Using special techniques, which achieve cooling rates of the order of 10^5 K s^{-1} [3], many metallic alloys readily form glasses, whereas unphysically high cooling rates, such as 10^{12} K s^{-1}, which can be generated on a computer, succeed in vitrifying even a simple liquid such as argon [11]. Perhaps the glass transition can thus be looked upon as a universal phenomenon that happens irrespective of the precise chemical nature of the liquid, provided the cooling rate is high enough.

The distinguishing property of this material may therefore not be the ability of a substance to form a glass, but rather the ease with which the solidification in a disordered liquid-like structure occurs. Among polymers, for instance, there are many substances that form glasses very easily, even when they are cooled with extremely slow cooling rates [3, 12]. Due to this intrinsic difficulty to crystallize, polymers are well suited for model investigations that concentrate on the universal features shared by all fragile glass formers [13], such as the non-Arrhenius behaviour of the viscosity or the time–temperature superposition property of the structural relaxation, as well as its strong stretching as compared to an ordinary Debye relaxation [1, 2, 9, 12]. Since for this kind of investigation the detailed microscopic structure of the polymers is not essential [14, 15] one can work with coarse-grained models that retain only basic properties of a polymer melt, such as chain connectivity and self-avoidance of the chains [16]. All of these models share the advantage that they can be simulated very efficiently, so that it is possible to obtain good statistics and to observe slow relaxation processes, which are especially prominent in the vicinity of the glass transition, over many decades in time. For instance, the bond-fluctuation model, originally proposed by Carmesin and Kremer [17], which is used in its three-dimensional version [18, 19] in this work, is such a model. The bond-fluctuation model is known to reproduce the expected static and dynamic behaviour of a dense melt in both two [20] and three dimensions [21] and it has been successfully applied to very diverse theoretical problems of polymer science, such as interdiffusion [18], the unmixing transition of

symmetric and asymmetric binary polymer mixtures [22], reptation dynamics [23, 24], layers of end-grafted polymer chains at surfaces [25], wetting phenomena [26] and the glass transition of two-dimensional polymer melts [27].

While the study dealing with the glass transition was done in two dimensions exclusively, and considered only a single cooling rate, the present work is a first step in extending this analysis to the three-dimensional case. In this paper we concentrate on the cooling-rate effects on the glass transition and on the structure of the frozen state. Starting from well equilibrated configurations at infinite temperature the melt was cooled continuously. We used fourteen different cooling rates covering two decades in time and 160 independent configurations each containing 1800 monomers, i.e. the statistics is based on 288 000 monomers in total. Combining this with an error analysis that carefully takes correlations into account, the statistical inaccuracy is well under control in this Monte Carlo simulation. Thus it is possible to obtain a rather precise estimate of the cooling-rate dependence of the freezing temperature of the melt, which is calculated in the standard way by the intersection point of two straight lines extrapolated from the liquid and glassy region [1, 3].

The contents of this paper are divided into the following parts. In section 2 we review the essential features of the bond-fluctuation model that are necessary for understanding our approach and we present the model Hamiltonian by which we want to introduce glassy behaviour in the *a priori* athermal system. This section also summarizes the simulation parameters and the cooling procedure. Section 3 deals with the results obtained for the temperature variation of characteristic quantities probing relevant length scales in the system; section 4 is exclusively devoted to a discussion of the cooling-rate dependence of the freezing temperature. The final section contains our conclusions, and gives an outlook on future work.

2. Model and simulation method

2.1. Bond-fluctuation method and the model Hamiltonian

The physical relevance of coarse-grained lattice models for polymers [16] is based on the idea that the long-distance and long-time properties of every flexible linear polymer chain can faithfully be represented by a 'Kuhnian chain' [14, 15]. Such a chain is usually constructed in the following way. One takes a certain number of chemical monomers adjacent to each other along the chain and lumps them together into one 'effective bead', which is then put in the centre of gravity of this group of chemical monomers. If one continues this coarse graining along the parent chain [28], the result is a set of effective beads distributed in space, which can then be connected by coarse-grained bond vectors [29]. Although the properties of these 'Kuhnian chains' largely depend upon the number of chemical monomers in the effective beads [29, 30], they all have in common the fact that the coarse-grained bond vectors and bond angles are very flexible. Choosing a chain length of ten effective beads then typically translates into an index of polymerization of 30–50 (for simple polymers such as polyethylene, for instance) [29, 30]. Contrary to the chemical bond vectors and bond angles, whose variations are largely limited by stiff potentials, they can fluctuate considerably. The bond-fluctuation model exploits this idea of the 'Kuhnian chain' and translates it onto a lattice [17, 18] (figure 1). In this spirit it is then completely natural that the energies characterizing the chemically realistic chain model (energies

for bond-length and bond-angle vibrations, torsional and non-bonded potentials) get 'mapped' onto effective potentials controlling the lengths of the effective bonds in the bond-fluctuation model (and possibly the angle between the bonds).

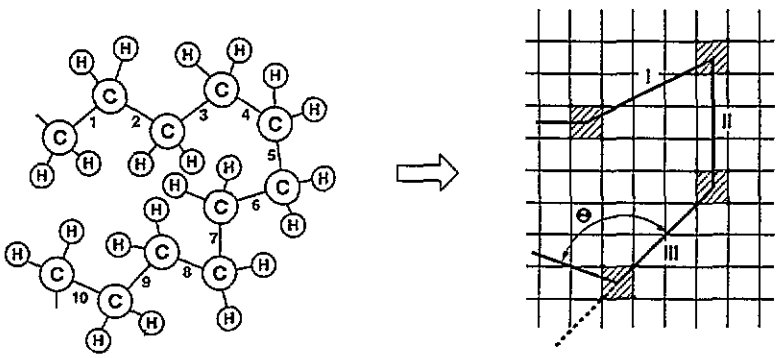

Figure 1. Schematic illustration of the construction of a coarse-grained model for a macromolecule such as polyethylene. In the example shown here, the subchain formed by the three C–C bonds labelled 1, 2, 3 is represented by the effective bond labelled as I, the subchain formed by the three bonds 4, 5, 6 is represented by the effective bond labelled as II, etc. In the bond-fluctuation model on the square (or simple cubic) lattice the length b of the effective bond is allowed to fluctuate in a certain range $b_{min} \leqslant b \leqslant b_{max}$, and excluded-volume interactions are modelled by assuming that each bond occupies a plaquette (or cube) of 4 (8) neighbouring lattice sites, which then are all blocked for further occupation.

In this model the polymer chains are represented by self- and mutually-avoiding walks (SAW) [16] on a simple cubic lattice where each monomer occupies a whole unit cell. The monomers are connected by bond vectors whose lengths are set to vary between two and $\sqrt{10}$ in three dimensions. The smallest length guarantees the local self-avoidance of the chains, whereas the largest length was chosen to be smaller than four in order to prevent the chains from crossing each other in the course of their motion. Using these restrictions on the bond lengths, six basic classes of bond vectors can be constructed, allowing 108 different bond vectors and 87 bond angles [18]. The basic bonds are

$$[2,0,0] \quad [2,1,0] \quad [2,1,1] \quad [2,2,1] \quad [3,0,0] \quad [3,1,0] \qquad (1)$$

where the symbol $[\bullet]$ stands for an equivalence class of bond vectors sharing the same length but differing in their direction. Thus the class $[3,0,0]$ comprises all bond vectors having a length of three and pointing in the positive and negative direction of the lattice axis. In the course of the Monte Carlo simulation a monomer is selected at random and moved for a lattice constant in an arbitrary direction, if the neighbouring lattice sites in the direction of the attempted move are empty (self-avoidance) and if the resulting new bond vectors belong to the classes of vectors enumerated above.

Note that, up until now, self-avoidance and the uncrossability of the walks are the only conditions that govern the chain dynamics. No Hamiltonian has yet been introduced to contribute to the motion of the monomers, and thus the model is still independent of temperature. The desired Hamiltonian should be designed in such

a way that it contains the basic microscopic ingredients of the physical phenomenon under study. Therefore the following question arises: what are these microscopic ingredients that bring about glassy behaviour? A hint for the answer to this question can be obtained from the theory of spin glasses [31]. From the study of these random magnetic systems it has been discovered that two properties are necessary to generate glassy behaviour, namely *frustration* and *randomness*. By randomness it is meant that the interaction between two spins is chosen according to some probability distribution so that they can either interact ferromagnetically or antiferromagnetically. But then a situation is conceivable where a spin cannot align in such a manner that it *simultaneously* satisfies all the energy requirements of its environment. This spin is said to be 'frustrated' [31].

If one assumes that frustration and randomness are in general responsible for the glass-like features of a system, one can try to incorporate them into the bond-fluctuation model. One way of doing that could look like this. Imagine that we assign an energy to each bond vector favouring those of the class [3,0,0] in comparison to all other vectors, i.e. we introduce the Hamiltonian

$$\mathcal{H}(b_{npc}) = \begin{cases} 0 & \text{if } b_{npc} \in [3,0,0] \\ \epsilon & \text{otherwise} \end{cases} \tag{2}$$

where b_{npc} *is the bond vector to the* n*th monomer of polymer* p *in configuration* c. Each bond will then try to stretch out along the lattice axis when the melt is cooled. But this stretching may be hindered by the presence of the other monomers in the neighbourhood of the specific bond. Therefore it is very likely that a competition arises between the attempt of a bond to adopt its energetically preferred state and the structural constraints that the surrounding monomers exert on that bond. If this competition prevents the system from satisfying the energy and geometry constraints simultaneously, a 'geometric frustration' may result (figure 2). Where this geometric frustration happens in the melt depends on the individual environment around a bond and can thus occur at very different (i.e. 'random') places in the system. Therefore the proposed two-level Hamiltonian very easily fulfils the above-mentioned requirements for glassy behaviour. Since all bond vectors of the class [3,0,0] are energetically favoured, irrespective of their orientation, a polymer can adopt many different configurations in its ground state. This large degeneracy of the ground state is also found in research on spin glasses, and is believed to be a characteristic trait of glass-forming substances [31].

As well as these arguments put forward in favour of the above Hamiltonian by analogy to the theory of spin glasses, one must also stress that it influences the properties of the lattice chains in a fashion similar to how a real chemical polymer behaves. If one decreases the temperature one increases the population of the 'trans' state [28] of an individual chemical bond. As a result, each real polymer will also try to expand if the melt is cooled [29,30], but the interaction with other chains may prevent, or at least hinder, this tendency. This feature is clearly apparent from various interesting attempts to realistically model the glass transition of polyethylene chains [32,33]. Our model thus captures, we think, the most important aspect of this behaviour, but it has the advantage that our simulations cover a range of times that extends over many decades (in units of the Rouse time [15] of the athermal high-temperature limit); by comparison, the time of the realistic simulations is less than a Rouse time due to the complexity of the structures that have to be considered explicitly. The proposed Hamiltonian therefore combines, in a natural way, both the

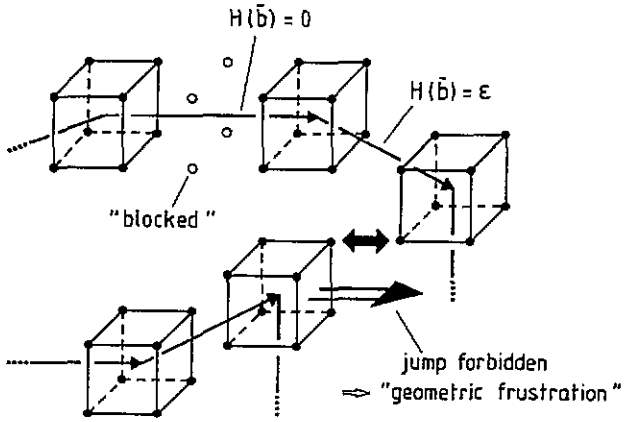

Figure 2. Sketch of a possible configuration of monomers belonging to different chains in the melt in order to illustrate the effect of the model Hamiltonian and the concept of geometric frustration. All bond vectors shown in this picture have an energy ϵ, except for the vector (3,0,0) which belongs to the ground state. This vector blocks four lattice sites (marked by o) that are no longer available to other monomers since two monomers may not overlap (the SAW condition). Due to this self-avoiding walk condition a jump in the direction of the large arrow is also forbidden. If a monomer tried to reach the ground state (i.e. a bond vector from the class $[3,0,0]$) by such a jump, the presence of the monomers in its surroundings would prevent this attempt (geometric frustration).

typical behaviour of a polymer melt during a cooling process and the major ideas of the very well established theory of spin glasses.

2.2. *Simulation parameters*

Naturally, this model Hamiltonian only develops its effect if the system is dense enough so that some of the bonds are 'frustrated'. What 'dense enough' actually means can be clarified if one calculates the critical density $\phi_c(N)$ above which the ground state is no longer accessible to the melt. Taking into account the special choice of the above-introduced Hamiltonian, a polymer consisting of N monomers on a d-dimensional lattice needs 2^d lattice sites per monomer and 2^{d-1} lattice sites per bond, i.e. it needs a total 'volume' of $N2^d + (N-1)2^{d-1}$ lattice sites in its ground state, so that the critical density is

$$\phi_c(N) = \frac{2^d N}{N2^d + (N-1)2^{d-1}} = 0.\bar{6} \times \frac{1}{1 - 1/(3N)} \xrightarrow{N\to\infty} 0.\bar{6} \quad \forall d. \tag{3}$$

Please note that this critical density, at which each lattice site is either occupied by a monomer or by a bond, varies only slightly with the degree of polymerization N ($\phi_c(3) = 0.75$, $\phi_c(10) = 0.69$). In this simulation a degree of polymerization $N = 10$ was chosen which guarantees that the melt at a density $\phi \geqslant 0.5$ exhibits 'Rouse dynamics' [34] without any complications caused by entanglement effects [14,15,21]. Since the relaxation times of the melt drastically increase with increasing chain length and density, it is advisable not to work at, or even above, the critical density for $N = 10$, especially if one takes into account the fact that the configurational constraints that prevent crystallization are much stronger in three dimensions than

in two [27]. Therefore a density between $\phi = 0.5$ and $\phi = 0.69$ was chosen for this simulation, i.e. $\phi = 0.5\bar{3}$, resulting from $\phi = 8NP/L^3$ with $N = 10$, the number of polymers per simulation box $P = 180$, and the length of one side of the box $L = 30$. Since periodic boundary conditions were used throughout the whole simulation to reduce the finite size of the system, a box length of $L = 30$ belongs to the lowest possible values where the radius of gyration is still smaller than half of this length for the whole temperature range (see section 4) so that the self-interaction of a chain with its periodic images becomes negligible. In total the simulation box contained 1800 monomers. In order to improve the statistics further, 160 independent configurations of this system were run, which was only possible because we worked with a highly optimized version of the bond-fluctuation algorithm [19]. While the individual simulation box thus contains only 3–4 times more particles than other recent glass simulations [35,36], our final results are based on particle numbers about 500 times larger than in the cited publications [35,36]. However, we feel that this large effort is indispensable for the questions studied in the present work. We performed an error analysis for all our data following the prescription given by Binder and Heermann [37], which allows us to obtain an accurate estimate of the error on correlated data. If not stated otherwise the statistical error is always of the size of the symbols in the following sections.

2.3. Cooling procedure

First, an initial configuration was generated by arranging the totally stretched polymers collinearly in layers. These layers were then superimposed and shifted with respect to each other in a random fashion in order to speed the subsequent relaxation, which was done at infinite temperature. We allowed the melt to relax until the chains had moved for a period of several (typically three) 'Rouse times' [15,21,23]. Starting from these well equilibrated athermal configurations the polymer melt was cooled from $T = \infty$ to $T = 0.05(= \beta_{\max}^{-1})$† by linearly changing the reciprocal temperature β as has already been done in two dimensions [27]:

$$\beta(t) = \beta_{\max}\Gamma_Q t. \tag{4}$$

Fourteen different cooling rates were simulated:

$$\begin{array}{lccccc} \Gamma_Q = & \underline{4.0 \times 10^{-5}} & 3.0 \times 10^{-5} & 2.0 \times 10^{-5} & 1.5 \times 10^{-5} & 1.0 \times 10^{-5} \\ & \underline{8.0 \times 10^{-6}} & 6.0 \times 10^{-6} & \underline{4.0 \times 10^{-6}} & 3.0 \times 10^{-6} & 2.0 \times 10^{-6} \\ & 1.5 \times 10^{-6} & 1.0 \times 10^{-6} & \underline{8.0 \times 10^{-7}} & \underline{4.0 \times 10^{-7}} & \end{array} \tag{5}$$

although it suffices to confine oneself to a smaller number of cooling rates in order to illustrate the general tendencies. Therefore only the cooling rates that have been underlined will be considered for most of the results presented in the following sections.

The above-specified cooling rates together with (4) show that the whole cooling process is done in 2.5×10^4 Monte Carlo steps (MCS) for $\Gamma_Q = 4 \times 10^{-5}$ and in 2.5×10^6 MCS for $\Gamma_Q = 4 \times 10^{-7}$, respectively. In order to get an impression of how the abstract Monte Carlo time unit, defined by the amount of time that is needed

† The temperature and all energies are measured in units of ϵ. All lengths are measured in units of the lattice constant.

to move each monomer once on average, can be related to conventional units of time one must take into account the fact that a monomer of the bond-fluctuation model stands for a group of chemical monomers of a real chain, as pointed out in the first paragraph of this section. Since this group typically contains about five chemical monomers for simple polymers such as polyethylene [29,30], for instance, the motion of a monomer in the bond-fluctuation model should correspond to bond reorientational jumps in the torsional potential of a real polymer whose relaxation time is of the order of 10^{-11} s. This identification, 1 MCS $\approx 10^{-11}$ s, is, however, only a rough estimate which may depend upon the choice of the model Hamiltonian. This fact is apparent from another study with the bond-fluctuation model, where the Hamiltonian was adapted in such a way that one could successfully simulate a real chemical polymer, namely bisphenol-A-polycarbonate [38]. In this simulation the good agreement between the calculated and experimentally measured values of the viscosity in the regime $\eta \leqslant 10$ poise allowed one to express the abstract Monte Carlo time unit in seconds. It turned out that one MCS corresponds to 1.5×10^{-13} s in this model, a value which is about two orders of magnitude smaller than the estimate from above. Using these approximate numbers one can conclude that the overall cooling process takes place in a time window of 10^{-12}–10^{-6} s, which is comparable to the time range of recent neutron scattering studies on polybutadiene [39].

3. Effects of the cooling rate

In order to obtain a deeper insight into the effects of the above-described geometric frustration and of the cooling rate, it is necessary to consider quantities that probe the relevant length scales of the system. There are already, *a priori*, two length scales of particular importance for an athermal polymer melt, namely the bond length and the radius of gyration. Quantities that are sensitive to changes on the first length scale are, for instance, the mean energy per bond and the 'Flory parameter'. They will be discussed in the following subsection.

3.1. Mean energy per bond and the Flory parameter

The mean energy per bond is defined as the average of the two-level Hamiltonian (2) over all bonds, polymers and configurations, i.e.

$$E_b(T) := \frac{1}{N-1} \sum_{n=1}^{N-1} \langle \mathcal{H}(b_{npc}) \rangle_{pc} \tag{6}$$

where the symbol $\langle \bullet \rangle_{pc}$ stands for

$$\langle \bullet \rangle_{pc} := \frac{1}{CP} \sum_{c=1}^{C} \sum_{p=1}^{P} \bullet_{pc} \tag{7}$$

with the explicit values $N = 10$, $P = 180$ and $C = 160$ from our simulation (see section 2). Since the temperature and all energies are measured in units of ϵ, the energy parameter in the model Hamiltonian (2), a bond can either adopt an energy of zero or one. If all bonds were in the excited state, the mean energy per bond would

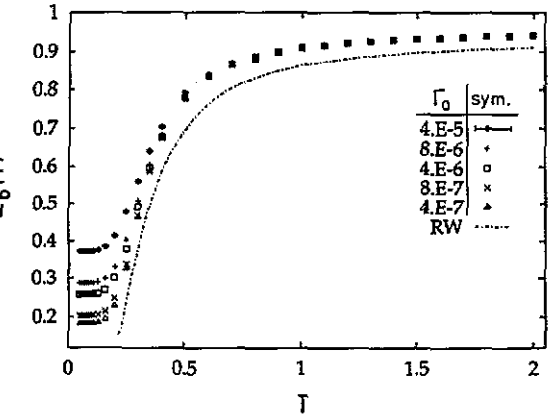

Figure 3. Plot of the mean energy per bond against T for five different cooling rates: $\Gamma_Q = 4.0 \times 10^{-5}$ (◇), $\Gamma_Q = 8.0 \times 10^{-6}$ (+), $\Gamma_Q = 4.0 \times 10^{-6}$ (□), $\Gamma_Q = 8.0 \times 10^{-7}$ (×) and $\Gamma_Q = 4.0 \times 10^{-7}$ (△). For the sake of clarity, error bars are only included for the first cooling rate (i.e. for $\Gamma_Q = 4.0 \times 10^{-5}$). The chain curve represents the random walk approximation of $E_b(T)$, equation (9).

have to be one, whereas it would become zero if all bonds populated the ground state, i.e. if frustration were absent. Therefore a non-vanishing value of the mean energy per bond at $T = 0$ serves as a good indication that the proposed Hamiltonian indeed introduces strong topological constraints.

Figure 3 shows a plot of $E_b(T)$ against T for the five representative cooling rates mentioned in section 2. In the high-temperature region ($T \in [0.6, 2.0]$) the value of $E_b(T)$ is close to one and the curves for the different cooling rates nicely collapse, emphasizing that the majority of the bonds are in the excited state and that the melt is mobile enough to adapt easily to the speed with which the temperature is changed. If one reduces the temperature further, more and more bonds go into the ground state until the curves level off in a narrow temperature range around $T \approx 0.2$. In this range the intrinsic relaxation times of the melt become comparable to the observation time, which is determined by the cooling rate. The system then falls out of equilibrium and gets locked at a value of E_b which therefore depends on the choice of the cooling rate. A further decrease of the temperature no longer influences the distribution of the bond vectors on the two energy levels. The melt is totally decoupled from the external 'heat bath' supplied by the Boltzmann factor. This decoupling will happen later for slower cooling rates, so the energy value where the curves get 'locked in' decreases with the cooling rate. Since $E_b(T)$ becomes constant as the temperature approaches zero it is clear that the anticipated geometric frustration effects are actually present, although we do not work at or close to the critical density (3). This, however, was necessary in two dimensions in order to develop similar effects [27], which indicates that the dimensionality of space might have a crucial influence on the glass transition, an influence that is well known from the research on spin glasses and Potts glasses [31,40]. Because of the present frustration effects we will refer to the low-temperature region ($T \leqslant 0.2$) as 'glass', whereas the above-specified high-temperature region is called 'liquid'.

In addition to the simulation data, a chain curve is shown in figure 3 that corresponds to a generalized random walk [16] approximation of the mean energy

per bond. A random walk approximation ignores all interactions among the bonds in the melt so that the partition function of a bond becomes identical to that of an isolated two-level system for our model Hamiltonian:

$$Z_{\mathrm{RW}}(\beta) = \sum_{b=1}^{108} \exp[-\beta(\mathcal{H}(b) + V_i)] \overset{V_i=0}{=} g_0 + g_\epsilon \exp(-\beta\epsilon) \tag{8}$$

where V_i stands for the total interaction potential of the dimer with the melt, and g_0 and g_ϵ are the degrees of degeneracy of the ground state and the excited state of a bond, respectively. Their values for the three-dimensional bond-fluctuation model are $g_0 = 6$ and $g_\epsilon = 102$. With these values, and the above-introduced partition function, it is now easy to calculate the mean energy per bond in the random walk approximation:

$$E_b^{\mathrm{RW}}(T) = \epsilon g_\epsilon \frac{\exp(-\beta\epsilon)}{Z_{\mathrm{RW}}(\beta)}. \tag{9}$$

Since the random walk approximation allows configurations where subsequent bonds are folded back on top of each other, the bond vector $(3,0,0)$ may be followed by the vector $(-3,0,0)$. Therefore the calculated mean energy per bond is systematically smaller than the simulation data. However, it is astonishing how close the result of this simple calculation lies with respect to the data that take full account of the self-avoiding walk condition. This property has already been observed in a different context [24].

The mean energy per bond only probes changes on the length scale of a bond. In order to go one step further one can search for a quantity that includes correlations between adjacent bond vectors. Such a quantity is the 'Flory parameter' or 'flexibility', $f(T)$, defined as the probability that the angle between two bond vectors ϑ_{npc} is not 180°:

$$f(T) := 1 - P(\vartheta_{npc}, T)|_{\vartheta_{npc}=180°}. \tag{10}$$

In this formula $P(\vartheta_{npc}, T)$ stands for the probability that the bond angle ϑ_{npc} is adopted at temperature T. Many years ago Flory tried to characterize the order–disorder phase transition in a melt with this flexibility [41] before Gibbs and diMarzio used his essential results to develop their theory for the glass transition of polymers [5, 42]. Thus it is of great interest to investigate this quantity near the glass transition. In figure 4 one can see a plot of this parameter against temperature.

Although $f(T)$ shows a similar dependence on the cooling rate as does the mean energy per bond, there are some distinct qualitative differences between the two quantities. In the high-temperature region ($T \in [0.6, 2.0]$) the mean energy per bond decreases much more strongly (by about 15%) than the amount of 180° angles increase (only about 0.2%). Therefore it seems that bond vectors that are in the ground state do not force their adjacent bond vectors to align with them. Correlations between the orientations of subsequent bond vectors are negligible in the high-temperature region, whereas they become significantly more important at intermediate temperatures between $T = 0.5$ and $T = 0.1$. In this temperature range the number of bonds in the ground state increases by a relative factor of 2–4 compared to the high-temperature region, while the same factor is about 20 times

larger for the 180° angle. The increase of the ground-state population thus induces a strong stretching of the bond angle, which is also clearly emphasized if one looks at the temperature dependence of the mean bond angle (figure 5). A further glance at the full bond-angle distribution function (which is not shown here) reveals that no other angle gains as much weight with decreasing temperature as the 180° angle does. This effect could not have been expected *a priori* from a Hamiltonian that only refers to the bond length and is independent of the individual orientation of the bond vector. Therefore it seems that this effect has to be considered as the result of a cooperative development of short-range static correlations.

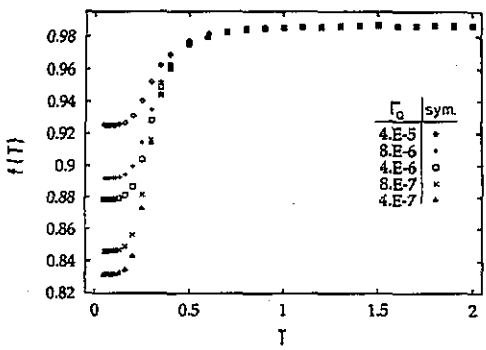

Figure 4. Flory parameter f against T for the five different cooling rates with the same choice as in figure 3. The errors are of the same size as shown for E_b and are therefore omitted.

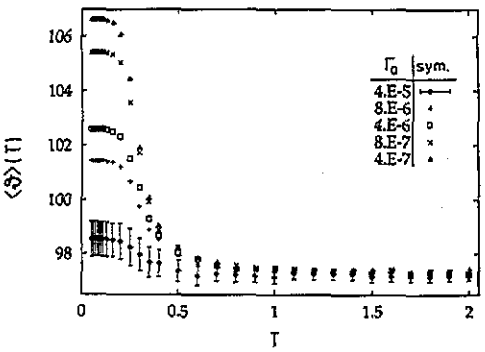

Figure 5. Plot of the mean bond angle for the five representative cooling rates with the same choices as in figure 3. Again, for the sake of clarity, the error bars are only shown for the fastest cooling rate.

3.2. *Specific heat and internal temperature*

If one knows the temperature dependence of the mean energy per bond one can define a specific heat per bond, C_b. As long as the system is in equilibrium C_b can be calculated either by the temperature derivative of $E_b(T)$ or by the application of the standard fluctuation relation from statistical mechanics [43]:

$$C_b := \frac{dE_b}{dT} \equiv \frac{1}{T^2}\langle(\mathcal{H}(b_{npc}) - E_b)^2\rangle_{npc}. \tag{11}$$

Here the symbol $\langle\bullet\rangle_{npc}$ represents the average over all bonds n, polymers p and configurations c, and is defined analogously to (7). If the system falls out of equilibrium the last equality no longer holds. This behaviour is exemplified in figure 6, which shows a comparison of the two ways of determining C_b for the fastest cooling rate $\Gamma_Q = 4.0\times10^{-5}$. In the high-temperature region ($T \geqslant 1.2$) there is no difference between the methods of calculating C_b. The melt is still in thermal equilibrium. However, as soon as the influence of the finite cooling rate makes itself felt the two curves no longer collapse. Whereas the specific heat calculated from the derivative of the energy exhibits the expected shape of a two-level system, i.e. a Schottky anomaly, C_b from the fluctuation relation steeply increases because the main temperature dependence comes from the prefactor in equation (11), i.e. $C_b \propto T^{-2}$, as the *energy*

fluctuations freeze together with the energy itself. The larger the cooling rate is, the earlier this increase happens (i.e. for $\Gamma_Q = 4.0 \times 10^{-5}$ around $T \approx 1.1$, and for $\Gamma_Q = 4.0 \times 10^{-7}$, not shown here, around $T \approx 0.7$) and is therefore clearly related to the onset of the above-mentioned decoupling of the melt from the external heat bath supplied by the Boltzmann factor. The external temperature then no longer coincides with the *internal temperature* T_i of the melt, which is reflected in the actual population of the two energy states. The concept of an 'internal temperature' distinct from the actual temperature below the glass transition has been widely used [1]. Therefore the following question arises: is it possible to assess, at least in an approximate sense, this internal temperature from the distribution function of the bond vectors on the allowed energetic states? Applying the random walk approximation again this can be tested in the following way:

$$\frac{N(\mathcal{H}(b_{npc}))}{N_b} = \frac{g_{\mathcal{H}} \exp(-\beta_i \mathcal{H}(b_{npc}))}{Z_{RW}(\beta)} \tag{12}$$

where $N(\mathcal{H}(b_{npc}))$ is the number of bond vectors having an energy corresponding to their state, $g_{\mathcal{H}}$ is the degree of degeneracy of the respective bond-vector energy (i.e. either 6 or 102, see the discussion below (8)) and N_b is the total number of bonds per configuration (i.e. $N_b = (N-1)P$). If one determines the bond-vector distribution function in the simulation, equation (12) is a first-order approximation of the temperature to which this distribution of bond vectors corresponds. For the actual definition of T_i the ratio of the probability of finding a bond in the ground state to that of finding it in the excited state was used, because the temperature-dependent partition function then cancels:

$$T_i := \left(\frac{1}{\epsilon} \ln \frac{g_\epsilon N(0)}{g_0 N(\epsilon)} \right)^{-1}. \tag{13}$$

Figure 7 shows a plot of the ratio T/T_i against temperature. If all interactions between the monomers had properly been taken into account in the calculation of T_i, the internal temperature would have been equal to the external temperature as long as the system was in equilibrium. However, instead of a horizontal line one finds a straight line with a finite slope in the high-temperature region, which must therefore be attributed to the neglect of the SAW condition. In the low-temperature glassy region the distribution of the bond vectors no longer changes, so that T_i becomes constant. Hence one expects to find a straight line with slope $1/T_i$ no matter which precise approximation was used to calculate T_i. This expectation is fulfilled, as a glance at figure 7 shows.

Despite the deficiency in the high-temperature behaviour, T_i can be used to replace the exploding prefactor in the fluctuation relation in order to assess the specific heat, which corresponds to the actual distribution of bond vectors. If one makes this replacement for all studied cooling rates one can hope to eliminate the history of the cooling, so that all specific heat curves should coincide if plotted against T_i. This elimination would correspond to a time–temperature superposition principle [1] for the cooling rate, a principle which is well known and very important in the dynamical analysis of the glass transition [2]. This expectation works out astonishingly well, as can be seen in figure 8. The specific heat data for the different cooling rates collapse nicely onto one single scaling curve, which can accurately be

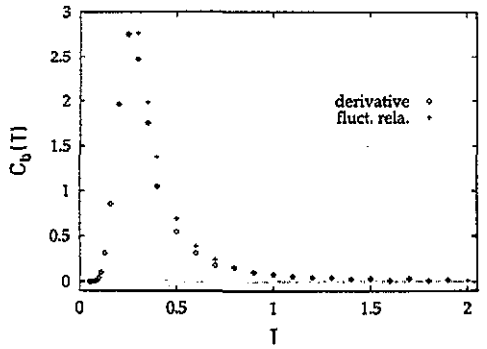

Figure 6. Comparison of the two ways of calculating $C_b(T)$ set out in (11) for the fastest cooling rate: the result of the derivative of $E_b(T)$ is marked by diamonds, whereas crosses correspond to the result of the fluctuation relation.

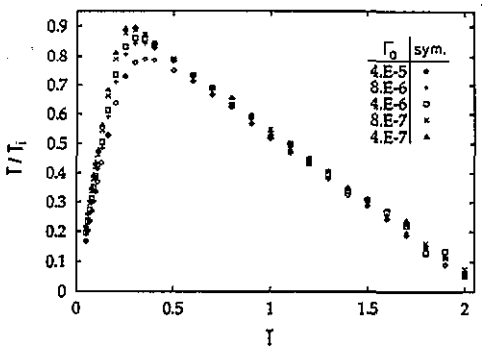

Figure 7. Plot of T/T_i against T for the five different cooling rates with the same choices as in figure 3.

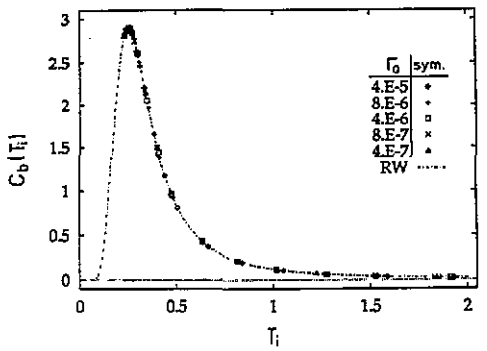

Figure 8. Plot of the specific heat against T_i for the five different cooling rates with the same choices as in figure 3. C_b was calculated by replacing T by T_i in the fluctuation relation of (11). The chain curve corresponds to the random walk approximation of $C_b(T)$ according to (14).

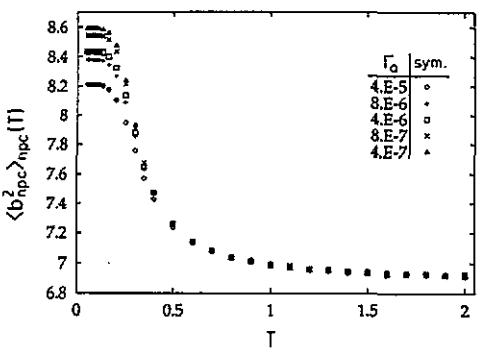

Figure 9. Mean squared bond length against temperature for the five representative cooling rates. The errors are of the same size as for E_b and have been omitted. The symbols have the same meaning as in figure 3.

described by the analytical expression of the specific heat for a two-level system. Using the partition function of the random walk again, equation (8), one obtains for $C_b^{RW}(T)$

$$C_b^{RW} = g_0 g_\epsilon \frac{(\beta\epsilon)^2 \exp(-\beta\epsilon)}{\mathcal{Z}_{RW}(\beta)^2}. \tag{14}$$

This result is shown as a chain curve in figure 8. We are currently studying whether the collapse of the specific heat data when rescaled by the above-introduced internal temperature, and the description of the resulting scaling curve by the two-level specific heat formula, are mere coincidences; or if it is indeed possible to reduce the complicated many-body interaction of the chains on a single-bond problem by virtue of a suitably defined internal temperature.

3.3. The mean squared bond length and the radius of gyration

In addition to the quantities discussed in the previous sections it is also worthwhile looking at a quantity like the mean squared bond length $\langle b^2_{npc}\rangle_{npc}$, which directly measures stretching on the length scale of a bond vector. The temperature dependence of $\langle b^2_{npc}\rangle_{npc}$ for the five representative cooling rates is very similar to that of the mean energy per bond (see figure 9). Following a high-temperature region (i.e. $T \in [0.6, 2.0]$), where the melt is in thermal equilibrium on the considered length scale for all cooling rates, the effect of the speed of cooling starts to be felt below $T \approx 0.5$, accompanied by a strong expansion of the mean bond length. The increase of $\langle b^2_{npc}\rangle_{npc}$ is stronger, by a factor of approximately two, than the decrease of $E_b(T)$ in the corresponding temperature range; exactly the opposite behaviour is observed in the high-temperature region. There $E_b(T)$ decreases by about 16% in comparison to only a 3% increase of $\langle b^2_{npc}\rangle_{npc}$. This difference can be rationalized in the following way. If a bond vector reaches its ground state it blocks $2^{(d-1)}$ lattice sites (see (3) and figure 2) which are no longer available for other monomers. This loss of 'volume' has to be compensated by a corresponding shrinking of other bond vectors in order to make the density stay the same. However, the compensation can only take place if the melt has enough time to overcome the energy barriers at the respective temperatures. It is certainly possible in the high-temperature region where the melt is still in equilibrium so that $\langle b^2_{npc}\rangle_{npc}$ only increases slightly, although many bonds adopt the ground state. But it will be progressively hindered the lower the temperature becomes and thus the more the finiteness of the cooling rate becomes visible. Since a bond vector can adopt a large mean squared bond length even though it is in the excited state (even 9 is possible by the equivalence class [2, 2, 1], see equation (1)) $\langle b^2_{npc}\rangle_{npc}$ increases much more steeply than $E_b(T)$ can decrease in the intermediate temperature range (i.e. $T \in [0.2, 0.5]$). The increase of $\langle b^2_{npc}\rangle_{npc}$ continues until the temperature reaches $T \approx 0.2$, where the curves level off and $\langle b^2_{npc}\rangle_{npc}$ gets locked at a value depending on the cooling rate. This final value of $\langle b^2_{npc}\rangle_{npc}$ in the low-temperature region is larger the slower the cooling rate is, but is always smaller than 9, which is the expected value for $\langle b^2_{npc}\rangle_{npc}$ in the ground state, a behaviour reminiscent of that of the mean energy per bond.

In addition to the scale of a bond another important length scale for a polymer is that of the radius of gyration. Therefore we also calculated this quantity, which is defined by

$$R^2_G = \frac{1}{N}\sum_{n=1}^{N}\langle(\boldsymbol{r}_{npc} - \boldsymbol{R}_{pc})^2\rangle_{pc} \tag{15}$$

where $\boldsymbol{r}_{npc}$ is the vector to monomer n in polymer p of configuration c, and $\boldsymbol{R}_{pc}$ is the vector to the centre of mass for the respective polymer. The result of the simulation is shown in figure 10. Qualitatively the dependence on temperature and on the cooling rate of the curves very much resembles that of the mean squared bond length. In the high-temperature range above $T = 0.5$ all five curves nicely collapse, proving that the melt is also in equilibrium on this length scale, whereas R^2_G increases steeply below $T = 0.5$ before it crosses over to a constant value in the temperature region where the melt vitrifies. Despite these qualitative similarities between the shapes of $\langle b^2_{npc}\rangle_{npc}$ and $R^2_G(T)$, a closer comparison of the two quantities reveals that R^2_G increases by the same amount (approximately 3%) as

the mean squared bond length in the high-temperature region, whereas at $T \leqslant 0.5$ the cooling rate crucially affects the strength of stretching on the two length scales. For $\Gamma_Q = 4.0 \times 10^{-5} \langle b^2_{npc} \rangle_{npc}$ expands faster than $R^2_G(T)$, whereas the opposite is true for $\Gamma_Q = 4.0 \times 10^{-7}$.

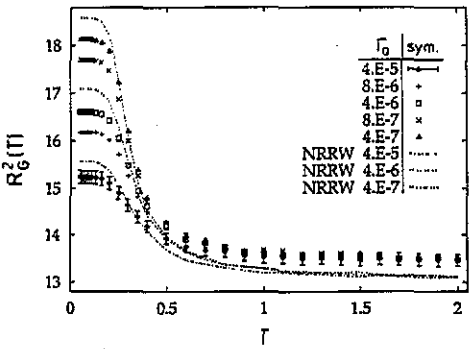

Figure 10. Radius of gyration against temperature for the five different cooling rates with the same choices as in figure 3. Error bars are again only included for the fastest cooling rate. The chain and broken curves correspond to the generalized non-reversal random walk (NRRW) approximation, which is explained in the text.

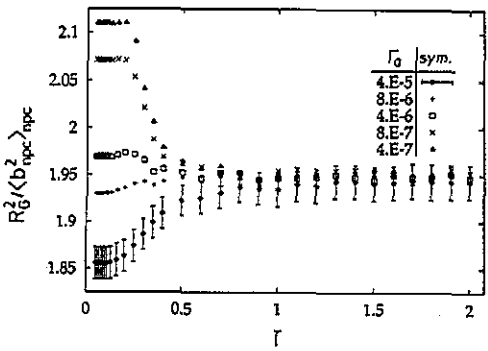

Figure 11. $R^2_G/\langle b^2_{npc} \rangle_{npc}$ against temperature for the five different cooling rates with the same choices as in figure 3. For the sake of clarity, error bars have only been included for the fastest cooling rate.

In order to illustrate this point further we compare our simulation data with a generalized non-reversal random walk (NRRW) [16] approximation of R^2_G, which can be obtained from a prescription that Flory describes in his textbook [28] if one uses the simulated bond-vector and bond-angle distribution functions to perform the necessary averaging [30]. Therefore this analytical calculation depends upon the details of the cooling process. The result of the approximation is also shown in figure 10, exemplified for three of the cooling rates. Since the NRRW approximation only partially takes into account the condition that no two monomers may overlap (the SAW condition) the calculated R^2_G values are systematically smaller than the simulated ones in the high-temperature region, because the self-avoidance of the monomers makes the polymer stiffer. However as soon as the influence of the cooling rate starts to be felt the NRRW approximation crosses the simulation data and settles down at a higher value of R^2_G in the glassy temperature region for all of the cooling rates. This *a priori* unexpected result can be rationalized as follows. Since the NRRW approximation only takes into account correlations between neighbouring bond vectors it is only affected by processes that happen on the local length scale of a bond. Changes on this length scale require a shorter amount of time than changes on a larger length scale, such as that of R^2_G, because more and more monomers are involved in the regrouping motion on larger length scales. *Hence different timescales belong to different length scales.* If the temperature is lowered very quickly only the local structure of the melt may be able to adapt to this speed, whereas the larger structures essentially remain in a state that corresponds to a higher (internal) temperature.

That these retardation effects, inferred only very indirectly from a comparison of the NRRW approximation and the simulation data, are actually present may be

visible if one plots the ratio of the radius of gyration and of the mean squared bond length, i.e. $R_G^2/\langle b_{npc}^2\rangle_{npc}$, against temperature for the different cooling rates. This is done in figure 11. It is clearly visible that the mean squared bond length expands faster than the radius of gyration if the cooling rate is large. The slower the cooling rate becomes the more R_G^2 catches up with the stretching of $\langle b_{npc}^2\rangle_{npc}$, until a cooling rate is reached where both length scales are affected in the same way (i.e. at $\Gamma_Q = 4.0 \times 10^{-6}$). For even smaller cooling rates the radius of gyration expands more strongly than the mean squared bond length due to the contribution of the bond angles to the overall size of the polymer.

4. Cooling-rate influence on the transition point

In the previous sections we have shown that the cooling rate strongly influences the temperature variation of different quantities that reflect the structure on the relevant length scales of the melt. All of these quantities can be used to determine the cooling-rate dependence of the freezing temperature T_g. This dependence is usually extracted from this kind of data by finding the intersection point of two straight lines, which are extrapolated from the glassy and liquid region, respectively [1,3,44]. Both of these straight lines are well defined for the internal temperature, where the interval $T \in [0.05, 0.09]$ was used for the extrapolation from the glassy region and that of $T \in [1.2, 2.0]$ for the liquid side. In the case of the 'S-shaped curves', like $E_b(T)$ or $R_G^2(T)$, however, a good choice for the temperature interval of the liquid region is not so evident. In order to find the centre of the curvature where these curves cross over to a constant value, the temperature interval $T \in [0.25, 0.35]$ was taken†. Although this interval lies deep down in the region of the undercooled liquid including only temperatures up to twice T_g, this is also the range conventionally used in experiments [1,3] and simulations [44] for the same analysis . In this way one can determine the cooling-rate dependence of the freezing temperature from $E_b(T)$ or $R_G^2(T)$ (as well as from the mean squared bond length, from the Flory parameter, the mean bond angle or the mean squared end-to-end distance of the chain, which is not shown here).

It turns out that all S-shaped curves yield similar results for this extrapolation, within the error bars, so that we confine ourself to the exemplification of the dependence of T_g upon the cooling rate by using two representative quantities, namely E_b and $\langle b_{npc}^2\rangle_{npc}$, for which the errors are smallest. The results of the extrapolation for E_b and for $\langle b_{npc}^2\rangle_{npc}$ are shown in figures 12 and 13, respectively, whereas the corresponding result derived from the internal temperature (i.e. from figure 7) is depicted in figure 14. Comparing these figures one can see at once that the cooling-rate dependence of T_g is strongly influenced by *the choice of the physical quantity* from which one determines it, and by the *size of the temperature interval* used for the extrapolation from the liquid side. None of these figures, however, shows the weak cooling-rate dependence of the freezing temperature usually found in experiments [1] where T_g decreases with falling cooling rate in proportion to the logarithm of Γ_Q. For the S-shaped curves T_g even *increases* for falling cooling rate before it becomes independent of it within the error bars below $\Gamma_Q \leqslant 6.0 \times 10^{-6}$, giving an average

† For the linear regression seven points were used in this interval, although for clarity only three are shown in the figures.

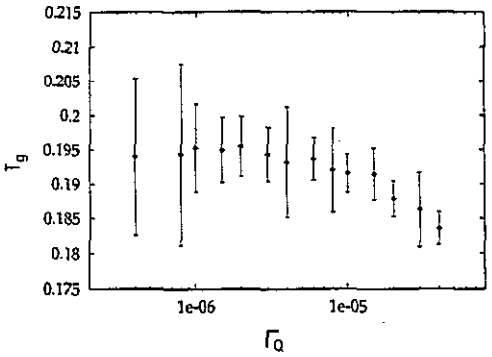

Figure 12. Freezing temperature T_g against Γ_Q obtained from the cooling-rate dependence of the mean energy per bond using all simulated cooling rates compiled in (5).

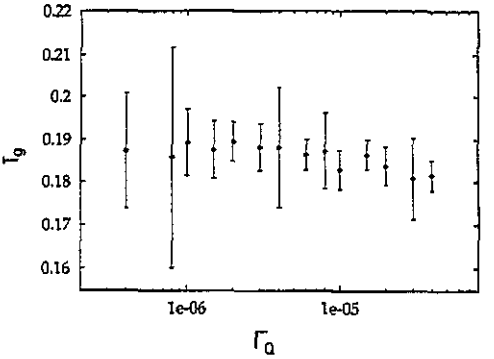

Figure 13. Freezing temperature T_g against Γ_Q obtained from the cooling-rate dependence of the mean squared bond length using all simulated cooling rates compiled in (5).

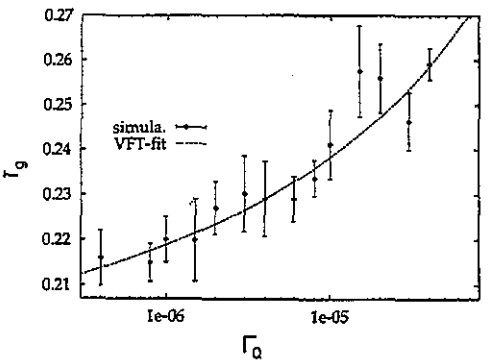

Figure 14. Freezing temperature T_g against Γ_Q obtained from the cooling-rate dependence of the internal temperature. The broken curve represents a non-linear fit to the data using (16).

freezing temperature of $\overline{T_{g,E}} = 0.194 \pm 0.003$ for $E_b(T)$ and of $\overline{T_{g,b}} = 0.188 \pm 0.004$ for $\langle b^2_{npc} \rangle_{npc}$, respectively. Since the two averages agree with each other within the error bars, one can combine them into a single average freezing temperature, which is representative for the S-shaped curves, i.e. $\overline{T_g} = 0.191 \pm 0.003$. Assuming that $T_g(\Gamma_Q)$ continues to fluctuate around this mean value for all cooling rates smaller than those studied, one can set $\overline{T_g}$ equal to the freezing temperature at an infinitely slow cooling rate T_K (i.e. $\lim_{\Gamma_Q \to 0} T_g(\Gamma_Q) =: T_K$). The abbreviation T_K for this limit has been chosen to remind us of the Kauzmann paradox mentioned in the introduction, which originates from a similar extrapolation procedure. T_K will therefore also be referred to as the Kauzmann temperature in the following. Contrary to that, the extrapolation for the internal temperature results in a non-linear relationship between T_g and $\ln(\Gamma_Q)$:

$$T_g(\Gamma_Q) = T_K + \frac{A}{\ln(B/\Gamma_Q)} \tag{16}$$

where T_K is defined above, and is a fit parameter like A and B. From the fit one obtains $T_K = 0.17 \pm 0.02$. The motivation to set up (16) is the experimentally well established Vogel–Fulcher law for the viscosity $\eta(T)$ [1] and the possible definition of the glass transition temperature as that temperature where the experimental observation time t_{exp} becomes comparable to the inherent relaxation times $\tau(T)$ [3] of the system. Using therefore the Vogel–Fulcher law with $\eta(T_g) \propto \tau(T_g) \stackrel{!}{=} t_{exp}$ and equation (4) one immediately arrives at (16). Although the extrapolated value of T_K from this non-linear fit coincides with the average freezing temperature of the S-shaped curves within its error bars, the deviation of the two T_K values shows that not only the functional relationship between T_g and Γ_Q, but also the limiting value of T_g for an infinitely slow cooling rate, is influenced by the size of the temperature interval chosen for the extrapolation from the liquid side. The larger this interval is the more accurate the result of the extrapolation should be. Therefore the T_K value from the internal temperature might be more reliable than that from the S-shaped curves. In addition, it also agrees very well with the Vogel–Fulcher temperature T_0, which can be obtained by fitting the Vogel–Fulcher law in the form

$$D(T) = D_\infty \exp\left(-\frac{C}{T - T_0}\right) \tag{17}$$

to the simulated temperature dependence of the chain's centre-of-mass diffusion coefficient. As well as T_0, D_∞ and C are fit parameters in the above equation. Since a detailed discussion of how the diffusion coefficient of the chains can be measured in a computer simulation and how its temperature dependence can be described by different empirical and theoretical laws will be given elsewhere [45, 46], we only present here the result of this analysis in figure 15 in order to show that the Vogel–Fulcher law succeeds in fitting the chain's diffusion coefficient over a large temperature range (i.e. $T \in [0.25, 0.8]$), resulting in a value of $T_0 = 0.17 \pm 0.02$, which agrees with the above-determined value of T_K within the error bars. Although these extrapolated glass transition temperatures, being derived from totally different physical quantities, are consistent with each other within numerical uncertainties, as is expected from experiment [5], one should always bear in mind that they stem from fitting procedures whose *validity* and *range of applicability* cannot be determined on a sound theoretical basis. Furthermore, the scale of the available time window for these extrapolations lies in the range of nanoseconds where the viscosity is typically about ten orders of magnitude smaller than at the calorimetric glass transition point. Certainly, extrapolations will become more and more unreliable the larger the range they have to cover, and it is thus conceivable that the determined values of T_0 or T_K are overestimated. Therefore, we feel that the real value of the extrapolation results for the Vogel–Fulcher and the Kauzmann temperatures is to stake out the interesting temperature region for a possible glass transition in our model and not to give a precise estimate of its absolute freezing point, although it was possible to reproduce the experimental value of the Vogel–Fulcher temperature up to an error of about 10% in the above-mentioned simulation of bisphenol-A-polycarbonate [38].

In view of these considerations, and of the above-obtained results, it seems that the experimentally observed linear relationship between T_g and $\ln \Gamma_Q$ might be a possible description of the influence of the cooling rate on the glass transition, but not necessarily the only one [47]. Whether or not it is found largely depends on the specific quantity under investigation and also on the range of studied cooling rates

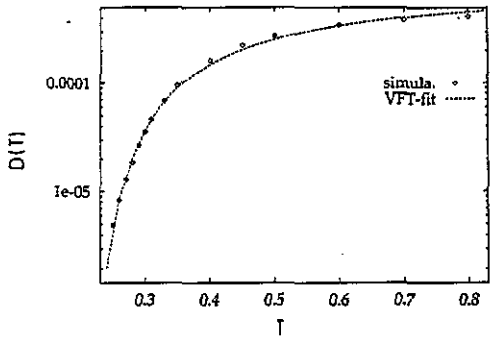

Figure 15. Plot of the diffusion coefficient against temperature. The broken curve corresponds to a non-linear fit with the Vogel–Fulcher law (17).

(for instance, for the range $\Gamma_Q \in [1.0 \times 10^{-6}, 1.0 \times 10^{-5}]$ in figure 14) because it predicts that T_g diverges as the cooling procedure approaches a quasistatic and thus thermodynamically well defined process. Therefore the linear relationship between T_g and $\ln \Gamma_Q$ should only be found if one confines oneself to a small range of cooling rates. The larger this range becomes the more the actual relationship should deviate from a linear relationship.

5. Conclusions and outlook

In this paper we have studied the cooling-rate dependence of the glass transition in a dense three-dimensional polymer melt by performing a Monte Carlo simulation with the bond-fluctuation model. Motivated by the theory of spin glasses, and the two-dimensional simulations for this system, we chose a simple two-level Hamiltonian to introduce a competition between the energetic demands of a bond and the topological constraints exerted on that bond by its environment. At low temperatures this competition results in a 'geometric frustration', where it is impossible that all bonds simultaneously adopt the energetically favourable ground state. Therefore the melt freezes in a highly disordered configuration whose structural properties depend on the applied rate of the cooling process. The influence of the cooling rate is exemplified by the temperature variation of various quantities that are sensitive to changes on both the local length scale of a bond and of the radius of gyration. It is shown that the cooling rate affects the structure on these length scales quite differently. The larger the length scale, the slower the cooling rate must be in order to allow the structure on this scale to adapt to the new temperature. Therefore the results of this simulation emphasize the idea that a typical relaxation time is connected with a specific length scale in the system.

If one tries to extract the cooling-rate dependence of the freezing temperature from the data one finds that the derived relationship is not unique, but that it largely depends on the quantity that is used for the analysis. Some of these quantities, such as the internal temperature, may produce a linear relationship between the logarithm of the cooling rate and the freezing temperature if one confines oneself to a small range of cooling rates (i.e. one decade in this simulation) whereas a larger range (two decades are already sufficient here) no longer exhibits this experimentally often-observed linear dependence and might rather be well described by a non-linear

Vogel–Fulcher-type behaviour. Other quantities, however, such as the mean energy per bond, may even show an increase of the freezing temperature with decreasing cooling rate before T_g approaches a constant value. This difference in the functional relationship of the freezing temperature with the cooling rate shows not only that the whole extrapolation procedure for determining T_K is very much influenced by the specific choice of the physical quantity, the size of the temperature intervals taken for the extrapolation and the way in which the melt is cooled (i.e. if one varies β linearly with time, as done here, or if one uses some other relationship between temperature and time), but it also emphasizes that *a unique freezing point* cannot unambiguously be defined as long as it is affected by the cooling rate. Since a cooling-rate dependent temperature may not be considered to be a 'temperature' from a strict thermodynamic point of view, only the quasistatic limit of T_g (i.e. $\lim_{\Gamma_Q \to 0} T_g(\Gamma_Q) = T_K$) might be a meaningful quantity. Therefore it is important that the studied range of cooling rates is large enough to perform this quasistatic limit. Nevertheless, the resulting values of this limit may still depend on the physical quantity under consideration and on the specific conditions under which the extrapolation has to be done. The mean energy per bond and the mean squared bond length, for instance, give a Kauzmann temperature of about $T_K \approx 0.19$, whereas the internal temperature leads to a value of about $T_K \approx 0.17$. Since the temperature interval on the liquid side is much larger for the latter quantity, the T_K result from the internal temperature might be considered as more reliable. Another argument in favour of this value for the Kauzmann temperature is that it is also consistent with the Vogel–Fulcher temperature derived from the diffusion data. Although the same fit function, namely different versions of the Vogel–Fulcher law, was applied to obtain T_K and T_0, this consistency of the values for the Kauzmann and Vogel–Fulcher temperature could not have been expected *a priori* because physical quantities of totally different origin were fitted. The coincidence of the two temperatures within the statistical errors, which was already pointed out by Adam and Gibbs [5], and the applicability of the Vogel–Fulcher law, should thus be interpreted as a confirmation that the bond-fluctuation method combined with the simple two-level Hamiltonian indeed reproduces experimentally well established features of the glass transition. This model Hamiltonian forces the melt to freeze in a liquid-like structure; the freezing does not take place at a well defined temperature (for a finite cooling rate) and it is accompanied by a drastic slowing down of the dynamics. The structure of the frozen melt really remains liquid-like, which can be studied by recording the coherent structure function which is sensitive to changes on *all* length scales in the system. Since the analysis made here was confined to the length of a bond vector and to that of the radius of gyration we will complete the investigation of the influence of the cooling rate on the glass transition by determining its effects on the structure function and on related quantities, and report the results in a separate publication [48].

Despite the above-stressed agreement of the Kauzmann and Vogel–Fulcher temperatures, one should not forget that they result from an extrapolation procedure for which neither the systematic error nor the theoretical justification is known. In view of these uncertainties it does not seem to us that a physically faithful extrapolation to an infinitely slow cooling rate is straightforwardly possible, so that all theoretical speculations based on such extrapolations must be doubtful. Hence we want to proceed in our analysis by allowing the configurations at certain temperatures to relax until the history of the cooling is eliminated. During this relaxation one can study the physical aging of the melt, while the equilibrated configurations at the end

of the relaxation may be used as starting points for further investigation of the static and dynamical aspects of the structural glass transition.

Acknowledgments

We thank the Höchstleistungsrechenzentrum (HLRZ) at Jülich for a generous grant of computer time on the Cray YMP. This work was supported by the Deutsche Forschungsgemeinschaft under grant number SFB 262. One of us (JB) is especially grateful to J Wittmer and H-P Deutsch for many helpful discussions, and to W Paul for many valuable comments during the preparation of this work and for a critical reading of the manuscript.

References

[1] Jäckle J 1986 *Rep. Prog. Phys.* **49** 171
[2] Götze W 1990 *Liquids, Freezing and the Glass Transition* ed J P Hansen, D Levesque and J Zinn-Justin (Amsterdam: North-Holland)
[3] Zallen R 1983 *The Physics of Amorphous Solids* (New York: Wiley)
[4] Kauzmann W 1948 *Chem. Rev.* **43** 219
[5] Gibbs J H and diMarzio E 1958 *J. Chem. Phys.* **28** 373, 807
Adam G and Gibbs J H 1965 *J. Chem. Phys.* **43** 139
[6] Crest G S and Cohen M H 1981 *Advances in Chemical Physics* ed I Prigogyne and S A Rice (New York: Wiley) p 445
[7] Fulcher G S 1925 *J. Am. Ceram. Soc.* **8** 339
[8] Kawasaki K 1970 *Ann. Phys.* **61** 1
[9] McKenna G B 1989 *Comprehensive Polymer Science* vol 2, ed C Booth and C Price (New York: Pergamon)
[10] Fredrickson G H 1988 *Ann. Rev. Phys. Chem.* **39** 149
[11] Fox J R and Andersen H C 1984 *J. Phys. Chem.* **88** 4019
[12] Sharples A 1972 *Polymer Science* vol 1, ed A D Jenkins (Amsterdam: North-Holland) ch 4
[13] Angell C A and Sichina W 1976 *Ann. NY Acad. Sci.* **279** 53
Angell C A 1988 *J. Phys. Chem.* **49** 863; 1991 *J. Non-Cryst. Solids* **191** 13
[14] de Gennes P G 1979 *Scaling Concepts in Polymer Physics* (New York: Cornell University Press)
[15] Doi M and Edwards S F 1986 *Theory of Polymer Dynamics* (Oxford: Clarendon)
[16] Kremer K and Binder K 1988 *Comp. Phys. Rep.* **7** 259
[17] Carmesin I and Kremer K 1988 *Macromolecules* **21** 2819
[18] Deutsch H-P and Binder K 1991 *J. Chem. Phys.* **94** 2294
[19] Wittmann H-P and Kremer K 1990 *Comp. Phys. Commun.* **61** 309; 1992 *Comp. Phys. Commun.* **71** 343
[20] Carmesin I and Kremer K 1990 *J. Physique* **51** 915
[21] Paul W, Binder K, Heermann D W and Kremer K 1991 *J. Phys.* **1** 37
[22] Deutsch H-P and Binder K 1992 *Europhys. Lett.* **17** 697; 1993 *Macromolecules* at press
[23] Paul W, Binder K, Heermann D W and Kremer K 1991 *J. Chem. Phys.* **95** 7726
[24] Wittmer J, Paul W and Binder K 1993 *Macromolecules* at press
[25] Lai P Y and Binder K 1991 *J. Chem. Phys.* **95** 9288
Lai P Y and Halperin A 1991 *Macromolecules* **24** 4981
Lai P Y and Zhulina E Z 1992 *J. Physique* **II2** 547
[26] Wang J S and Binder K 1991 *J. Chem. Phys.* **95** 8537; 1992 *Makromol. Chem., Theory Simul.* **1** 49; 1991 *J. Physique* **I1** 9288
[27] Wittmann H-P, Kremer K and Binder K 1992 *J. Chem. Phys.* **96** 6291
[28] Flory P J 1969 *Statistical Mechanics of Chain Molecules* (New York: Wiley)
[29] Baschnagel J, Binder K, Paul W, Laso M, Suter U W, Batoulis I, Jilge W and Bürger T 1991 *J. Chem. Phys.* **95** 6014
[30] Baschnagel J, Qin K, Paul W and Binder K 1992 *Macromolecules* **25** 3117

[31] Binder K and Young A P 1986 *Rev. Mod. Phys.* **58** 801
[32] Roe R-J, Rigby D, Furuya H and Takeuchi H 1992 *Comp. Polym. Sci.* **2** 32
[33] Clarke J H R and Brown D 1986 *Mol. Phys.* **58** 815; 1989 *Mol. Simul.* **3** 27
[34] Rouse P E 1953 *J. Chem. Phys.* **21** 1272
[35] Wahnström G 1991 *J. Non-Cryst. Solids* **131–3** 109
[36] Loewen H, Hansen J P and Roux J-N 1991 *Phys. Rev.* A **44** 1169
[37] Binder K and Heermann D W 1988 *Monte Carlo Simulation in Statistical Physics: An Introduction* (Berlin: Springer)
[38] Paul W 1992 *AIP Conf. Proc.* **256** 145
[39] Richter D, Zorn R, Farago B, Frick B and Fetters L J 1992 *Phys. Rev. Lett.* **68** 71
Frick B, Farago B and Richter D 1990 *Phys. Rev. Lett.* **64** 2921
Richter D, Frick B and Farago B 1988 *Phys. Rev. Lett.* **61** 2465
[40] Scheucher M, Reger J D, Binder K and Young A P 1990 *Phys. Rev.* B **42** 6881
[41] Flory P J 1956 *Proc. R. Soc.* A **234** 60; 1982 *Proc. Natl Acad. Sci.* **79** 4510
[42] Wittmann H-P 1991 *J. Chem. Phys.* **95** 8449
[43] Huang K 1963 *Statistical Mechanics* (New York: Wiley)
[44] Angell C A, Clarke J H R and Woodcock L V 1981 *Advances in Chemical Physics* ed I Prigogyne and S A Rice (New York: Wiley) p 397
[45] Baschnagel J, Wittmann H-P, Paul W and Binder K 1993 *Trends in Non-Crystalline Solids* ed A Conde, C F Conde and M Millán (Singapore: World Scientific)
[46] Baschnagel J and Binder K 1993 to be published
[47] Brüning R and Samwer K 1992 *Spring Conf. of the German Physical Society* (Weinheim: Physik)
[48] Baschnagel J and Binder K 1993 *Physica* A submitted